



# International Journal of Pharmacology

ISSN 1811-7775

**science**  
alert

**ansinet**  
Asian Network for Scientific Information

## Research Article

# Chronic Stress Promotes Epithelial-Mesenchymal Transition in Lung Carcinogenesis Through the Induction of TGF-1

\*<sup>1,2</sup>Yitian Chen, \*<sup>1</sup>Zuanjun Su, <sup>3</sup>Bo Tang, <sup>1</sup>Jinming Cao, <sup>1</sup>Zhicong Chen, <sup>1</sup>Weijia Cai, <sup>1</sup>Canye Li, <sup>2</sup>Zhijun Guo, <sup>4</sup>Jian Cai, <sup>1</sup>Ting Zhou and <sup>1</sup>Feng Xu

<sup>1</sup>Fengxian Hospital, Southern Medical University, Shanghai, China

<sup>2</sup>Heyou International Hospital, Shunde, Guangdong, China

<sup>3</sup>Nanhai Fifth People's Hospital, Foshan, Guangdong, China

<sup>4</sup>Fengxian Mental Health Center, Shanghai, China

\*These authors contributed equally

## Abstract

**Background and Objective:** Chronic stress promotes tumor progression but the specific mechanism in the sympathetic nervous system is unclear. To explore the mechanism of whether chronic stress affects hormone levels and thus tumor progression, this study was conducted. **Materials and Methods:** A tumor-bearing mouse model was constructed by inoculating tumor cells and depression-like phenotype by chronic unpredictable mild stress, CUMS. The A549 cells were exposed to stress hormones. Mice were divided into 4 groups (n = 8): Control group, Tumor group, CUMS group and Tumor+CUMS group. Detecting the changes of mice models of tumor, CUMS and Tumor+CUMS in serum hormone and molecules of epithelial-mesenchymal transformation (EMT) in tumor tissues. The change of molecules of EMT when exposing A549 cells to cortisol and norepinephrine. **Results:** Chronic stress led to the increase of serum corticosterone and noradrenaline and enhanced the metastasis and invasion of cancer cells. *In vivo* chronic stress resulted in increased expression of tumor TGF- $\beta$ 1 and the changes of EMT-related molecules were also consistent with its course. *In vitro*, A549 cells showed morphological changes under CORT and NE, enhanced cloning, migration and invasion ability, up-regulated the expressions of TGF- $\beta$ 1, N-cadherin and Vimentin, down-regulated E-cadherin and ZO-1. The opposite phenomenon occurred after knocking down TGF- $\beta$ 1. However, CORT and NE reversed these changes. **Conclusion:** The high stress hormone levels caused by chronic stress affected the expression of TGF- $\beta$ 1 and thus promoted the tumor EMT.

**Key words:** Chronic stress, lung tumor, stress hormone, TGF-1, epithelial-mesenchymal transition

**Citation:** Chen, Y., Z. Su, B. Tang, J. Cao and Z. Chen *et al.*, 2023. Chronic stress promotes epithelial-mesenchymal transition in lung carcinogenesis through the induction of TGF-1. *Int. J. Pharmacol.*, 19: 673-690.

**Corresponding Author:** Jian Cai, Fengxian Mental Health Center, Shanghai, China

Ting Zhou and Feng Xu, Fengxian Hospital, Southern Medical University, Shanghai, China

**Copyright:** © 2023 Yitian Chen *et al.* This is an open access article distributed under the terms of the creative commons attribution License, which permits unrestricted use, distribution and reproduction in any medium, provided the original author and source are credited.

**Competing Interest:** The authors have declared that no competing interest exists.

**Data Availability:** All relevant data are within the paper and its supporting information files.

## INTRODUCTION

Depression is an emotional disorder that always shows negative emotions such as loss of interest<sup>1,2</sup>. According to the World Health Organization (WHO), depression is the third leading disease in the world, affecting an estimated 350 million people worldwide and is projected to be the number one disease burden by 2030<sup>3</sup>. Many factors, such as psychosocial stress and biological stress, are involved in the pathogenesis of depression and may cause depression through different pathologic mechanisms<sup>4,5</sup>.

In recent years, the incidence of malignant tumors has been on the rise. Lung cancer is the most common cancer and the leading cause of cancer death<sup>6</sup>. Non-Small Cell Lung Cancer (NSCLC) is the most common type of lung cancer. It accounts for more than 80% of lung cancer cases<sup>7,8</sup>.

The incidence of depression in patients with cancer is 15-29%, which is 3-5 times higher than that in patients without cancer<sup>9,10</sup>. A series of studies at home and abroad have shown that psychosocial stress can affect the occurrence, development and metastasis of cancer<sup>11</sup>. Cancer patients have a high risk of depression comorbidity, which will bring more subjective pain to patients, affect physical treatment and rehabilitation, reduce the quality of life, accelerate tumor progression and lead to higher tumor-related mortality<sup>12</sup>. Previous research has also indicated that stress-related factors such as marital status, taking analgesic or anxiolytic drugs are relevant to promoting cancer progression<sup>13</sup>. Therefore, an in-depth understanding of the potential mechanisms by which chronic stress contributes to cancer progression can help prevent and forestall the negative effects of chronic stress on it.

Chronic psychological stress can induce continuous activation of the sympathetic nervous system (SNS) and the Hypothalamic-Pituitary-Adrenal (HPA) axis. The SNS mainly mediates the secretion of catecholamines, including norepinephrine (NE) and epinephrine (E) and promotes tumor growth mainly by acting on  $\beta$ -Adrenalin Receptors ( $\beta$ -ARs). The activation of the HPA axis affects tumor progression mainly through the release of glucocorticoid (GC). When the body is subjected to stressful stimuli, there is an increase in cortisol synthesis, which in turn leads to a number of "alert" reactions in the body. In this case, the hypothalamus releases a series of hormones such as corticotropin (CRH) and arginine vasopressin (AVP), which further activate the pituitary and adrenal cortex to release Adrenocorticotrophic Hormone (ACTH) and the glucocorticoid cortisol (CORT) and so on, exposing the immune system to high stress hormone levels, which can affect cancer progression by weakening innate and adaptive immunity<sup>14-17</sup>.

Epithelial-to-mesenchymal transition (EMT) is a crucial molecular mechanism mediating metastatic progression, which drives the malignant progression of several cancers<sup>18-20</sup>. Among the many secreted growth factors and cytokines, the Transforming Growth Factor- $\beta$  (TGF- $\beta$ ) family has received much attention for its multiple functions at the cellular level and during development, as well as its role in a variety of diseases, including cancer. Loss of control of the TGF- $\beta$  family signaling can lead to developmental abnormalities and disease, while increased signaling of TGF- $\beta$ 1 often leads to cancer and fibrosis. Increased expression of TGF- $\beta$ 1 is a key factor in EMT and increased TGF- $\beta$ 1 signaling in cancer cells makes cancer cells more aggressive<sup>21-23</sup>. The TGF- $\beta$ 1 signaling pathway is involved in tumorigenesis and metastasis, suggesting that it is a promising target for cancer therapy.

In the previous experiments, noradrenaline and cortisol levels were elevated in depressed-like phenotype mice<sup>24,25</sup> and the tumor growth was faster and the tumor volume was larger in the depression-like phenotype group than tumor comorbid depressive mice<sup>13,26</sup>, leading to the hypothesis that the tumor progression was influenced by changes in NE and cortisol in the internal environment during depression. However, the mechanism how these serum hormone changes affect cancer is not clear. It was also hypothesized that depression-induced increases in serum norepinephrine and cortisol promote EMT progression in tumor cells by up-regulating the expression of TGF- $\beta$ 1.

## MATERIALS AND METHODS

**Study area:** This study was conducted from February, 2021 to December, 2022 in Fengxian Hospital, Southern Medical University, Shanghai, China.

### Materials

**Cell culture:** Human non-small cell lung cancer cell (A549) and murine non-small cell lung cancer cells (LLC) were obtained from the National Collection of Authenticated Cell Cultures (Shanghai, China). All cell lines were cultured in a humidified incubator (Thermo, America), with 5% CO<sub>2</sub>, at 37°C and supplemented in DMEM with 10% fetal bovine serum (FBS, Gibco, America) and 1% antibiotics (NCM Biotech, Suzhou, China). The NE (N-069, 100  $\mu$ g mL<sup>-1</sup>, Sigma, America) and CORT (C-106, 1.0 mg mL<sup>-1</sup>, Sigma, America) solutions were diluted to 100  $\mu$ M NE and 10  $\mu$ M CORT with DMEM containing 10% de-hormone serum and used in subsequent cell experiments.

**Model mice:** Thirty-two male C57BL/6 mice (weighted 20-22 g) without gene modification were taken from Huachuang Sino Experimental Animal Co. Ltd. (Animal Quality Certificate: 2022038233) and housed in the Specific Pathogen Free SPF laboratory animal center. The animals used in this study have been prepared in accordance with national laws and regulations on animal care. The animal experiment protocol was approved and filed with the Bioethics Committee of Fengxian Hospital (approval number: 22010737).

## Methods

**Group and molding protocols:** Mice were fed at a controlled room temperature  $20\pm2^{\circ}\text{C}$ , normal day and night environment and unlimited water and diet for mice. After 1 week of animal adaptation, behavioral tests were performed on the mice, including sucrose preference test and open field test. The mice meeting the requirements were randomly divided into 4 groups by random number method ( $n = 8/\text{group}$ ): Group A (Control group), group B (Tumor group), group C (CUMS group) and group D (Tumor+CUMS group). As  $5\times10^4$  LLC cells were suspended in 0.2 mL normal saline and injected subcutaneously into the hind limbs of mice in group B and D to induce tumor. Mice in group A and B were not given any stimulation and ate and drank normally. Mice in group C and D were fed in a single cage and given chronic unpredictability mild stress (CUMS)<sup>27-29</sup> for 6 weeks. Stressors included swimming in 40/4 water for 3 min, behavioral restriction for 3 hrs, day/night reversal for 24 hrs, night light for 12 hrs, noise stimulation for 1 hr, cage shaking for 15 min, cage tilt at  $45^{\circ}\text{C}$  for 24 hrs, wet bedding for 24 hrs and empty cage for 24 hrs. During modeling, two or three stressors were randomly administered daily, with each stimulus applied an average of two to three times per week. In order to prevent the animal from anticipating the occurrence of the stimulus, the same stimulus cannot be applied consecutively. After 6 weeks, the sucrose preference test, open-field test, forced-swimming test and tail-suspension test were used to verify the success of depression model.

**Sucrose preference test (SPT):** The sucrose preference test was used to detect depressive anhedonia in mice<sup>30</sup>. Mice were given a bottle of drinking water and a bottle of 1% sucrose water 24 hrs before the experiment and the locations of drinking water and sucrose water were exchanged 1 hr later and again 1 hr later. After the adaptation of sucrose water for 24 hrs, the intake of drinking water and sucrose water of mice for 24 hrs was recorded and the percentage of sucrose water preference was calculated according to the liquid consumption. The experiment on sucrose preference was

performed on mice before and after modeling and the results were helpful in judging the success of the depression model in mice:

$$\text{Sucrose water preference (\%)} = \frac{\text{Sucrose water consumption}}{\text{Total liquid consumption}} \times 100$$

**Open-field test (OFT):** The experimental device was composed of open field and data acquisition and processing system (ZSZRDC Science and Technology Co. Ltd., China). The open field was  $100\times100\times40$  cm, the inner wall was painted black, the bottom board was white board and it was divided into four grids of  $50\times50\text{ cm}^2$ , which could monitor the behavior of four mice at the same time. The peripheral area ( $50\times50\text{ cm}^2$ ) and the central area ( $30\times30\text{ cm}^2$ ) were delimited for each open field. The experiment should be carried out in a quiet environment with proper light and humidity. Mice were placed in the central part of the bottom surface of the open field and their behavior tracks were collected after 1 min of adaptation and the collection time was 5 min. Behavioral detection parameters included the number of times mice entered the peripheral and central areas, residence time, exercise distance and total exercise distance etc.

**Forced-swimming test (FST):** Mice were placed in a transparent bucket with a diameter of 110 mm  $\times$  a height of 300 mm. During the test, a water level of  $37^{\circ}\text{C}$  was added to the bucket to a water level of 20 mm, which provided an unavoidable compression environment and the time of immobility in water was measured by the instrument. The duration of recording was 5 min and the last 4 min was selected as the exercise condition of mice. The parameters of forced usefulness were immobility time, immobility times and activity time.

**Tail-suspension test (TST):** The experimental device is composed of a suspension box and a data acquisition and processing system. When the mice were suspended in a square box 30 cm from the ground, the stationary time of the mice was collected and recorded for a total of 5 min. The last 4 min was selected as the movement of the mice. The test parameters of the tail suspension test included stationary time, stationary times and activity time of mice.

**ELISA measurement of NE and corticosterone:** The levels of NE and corticosterone in serum were assessed using ELISA kits (NE ELISA kit, Biovision, ab287789, corticosterone ELISA kit, KGE009) according to the operating guide.

**Hematoxylin-eosin and staining (H&E):** Mice tissues, including liver and lung tissues, were collected and placed in 4% paraformaldehyde for tissue fixation. The fixed tissue was paraffin embedded and sliced. Paraffin sections were successively placed into xylene for 20 min, xylene for 20 min, anhydrous ethanol for 5 min, anhydrous ethanol for 5 min, 75% alcohol for 5 min and finally washed with tap water to dewax the paraffin sections. Then the slices were put into the hematoxylin dye solution for 3-5 min, washed with tap water, differentiated liquid differentiation, washed with tap water, followed by blue return solution, rinse with running water. The sections were dehydrated with 85% gradient alcohol and 95% gradient alcohol for 5 min, respectively and then stained with eosin dye solution (Yuxiu Biotechnology, Shanghai, China) for 5 min. Last, a microscope (Olympus Corporation, Japan) was used for photography.

**Cell transfection:** Inoculate  $1 \times 10^5$  A549 cells individually in 6-well plates 24 hrs in advance and knock down TGF- $\beta$ 1 using siRNA targeting (Gene primer sequence of siTGF- $\beta$ 1, sense: GCAGAGUACACACAGCAUATT, Antisense: UAUGCUGUGUG UACUCUGCTT). Incubate siRNA and transfection reagent Lipo3000 (Thermo, America) with Opti-MEM medium (Gibco, America) separately for 5 min and then mix and incubate for 20 min to form liposome-siRNA complexes. Finally, they were added to the lined 6-well plates and the cells could be collected after 48/72 hrs.

**Cell viability assay by CCK-8:** The A549 cells were inoculated with 100  $\mu$ L ( $1 \times 10^3$  cells) per well in a 96-well plate and when the cells were plastered after 12 hrs, the medium was replaced with de-hormone medium for hormone starvation and subsequently replaced with norepinephrine solution (0, 0.1, 1, 10, 20, 50 and 100  $\mu$ M) and cortisol solution (0, 1, 1.5, 2 and 5  $\mu$ M) were added to the wells at 37°C. As 10  $\mu$ L of Cell Counting Kit-8 (CCK-8) reagent was added to each well and the absorbance (OD) at 450 nm was measured on a full wavelength enzyme standardizer (Bio Tek, America) after incubation for 1-4 hrs at 37°C in an incubator protected from light. The OD of each well was deducted from the blank control wells and then compared to analyze the cell activity.

**Cell morphology:** The A549 cells were inoculated in 48-well plates with 200 cells per well, cultured for 12 hrs for serum-starved and then cultured with 1.5  $\mu$ M CORT for 24 hrs and 10  $\mu$ M NE for 48 hrs, stained for cell estimates using fluorescent substances FITC Phalloidin (100 nM) (CA1620, Solarbio, Beijing, China) and the nuclei were re-stained with

DAPI (C0060, Solarbio, Beijing, China) stain, followed by observation and photography under fluorescence microscope (Olympus Corporation, Japan), selecting FITC excitation/emission filter (Ex/Em = 540/570 nm) and DAPI excitation/emission filter (Ex/Em = 364/454 nm) at the same screen for taking pictures.

**Clone formation assay:** The A549 cells were inoculated into 6-well plates at a density of  $1 \times 10^3$  cells per well and incubated for 10-14 days after 12 hrs with serum starvation in de-hormone medium with 10  $\mu$ M NE and 1.5  $\mu$ M CORT, changing the medium every three days. When the number of cells in a single clone is greater than 50 as observed under the microscope, 4% paraformaldehyde can be used for fixation and crystalline violet staining operation and then dried and photographed under the microscope.

**Wound healing assay:** The A549 cells were inoculated into the marked 6-well plates at a density of  $1 \times 10^6$  cells per well and serum starvation was performed 12 hrs later. Sterile 200  $\mu$ L pipette tips were used to make wounds in the cell layer and then the cells were washed with PBS twice, 2 mL 10  $\mu$ M NE and 1.5  $\mu$ M CORT was added. The visual field was selected under the microscope to observe and take pictures (0, 24 and 48 hrs after the scratch) and the horizontal mobility of cells was calculated.

**Cell migration assay:** The A549 cells (or with si-TGF- $\beta$ 1) were digested and resuspended in serum-free medium at a concentration of  $2.5 \times 10^5$  cells  $\text{mL}^{-1}$ . The transwell chamber was placed in the filling well. As 10  $\mu$ M NE 600  $\mu$ L and 1.5  $\mu$ M CORT 600  $\mu$ L was added into the chamber (lower chamber) and 200  $\mu$ L cell suspension was slowly added into the chamber (upper chamber). The transwell chamber was cultured at 37°C for 8 hrs. After the cell culture was completed, appropriate amount of 4% paraformaldehyde was added to fix the cells on the surface of the subventricular membrane for 30 min. Add 0.1% crystal violet and stain for 30 min. The cells on the bottom of the chamber were gently wiped with cotton swabs, washed in water to remove the wiped cells and after drying, 5 fields were selected for each chamber under the microscope to take photos and the number of cells passing through the membrane of the chamber was calculated and counted.

**Cell invasion assay:** The cell was coated with Matrigel (Corning, 354234) 4 hrs in advance and the other steps were the same as the cell migration assay.

Table 1: Primer sequences of all genes

Gene	Forward	Reverse
GAPDH (Mus)	GACATGCCGCCCTGGAGAAC	AGCCCAGGATGCCCTTAGT
TGF- $\beta$ 1 (Mus)	GCAACAATTCTGGCGTTA	ATGCTCTGGCAGAGTGAGA
E-cadherin (Mus)	GCCTTGCTTCAGGGCGTC	TTGCTGACCTCTGAGGC
N-cadherin (Mus)	GGAGATTTATGCGGACGG	CACCATGGCAATGAGCGGTT
Vimentin (Mus)	GGCCAGATCCTGTCCAAGC	TACCCCTGGTGGTTAAGCTG
ZO-1 (Mus)	ATGGGAATGAAACTTGATGGC	GGCGAGGAGAGCAGGATTTC
$\beta$ -ACTIN (Homo)	GAAATACCTGACGGTGCTC	TTCCGTCCTCTGGTTCAG
TGF- $\beta$ 1(Homo)	TGGAGCTTAGATGCCGTT	CATTGAGAAGGGCTGTCCTT
E-cadherin (Homo)	CTCCAGGGACTCGTTAGTGC	CCATTGCTGTGCTTAGCG
N-cadherin (Homo)	AGGTCTTGCGGATGCCACGT	GTGGGTTCCACCATAGCAC
Vimentin (Homo)	CAAATCCAAGCCGTGGTG	CAGTTGCTAAACTCACTGAAAGG
ZO-1 (Homo)	TGGGTATCAACCAGAGGGAGT	GAGGATGGCGTACCCACAG

**Determination of EMT relative gene mRNA expression:**

Total RNA was extracted from mouse tissues and cells using TRIzol extraction reagent and the RNA was reverse transcribed to cDNA according to the instructions of the reverse transcription reagent. For qRT-PCR, TliRNaseH Plus was used according to the manufacturer's protocol. The primers sequences were shown in Table 1.

**Western blotting analysis of EMT relative proteins:** The mice tissues (included tumor and liver) and A549 cells were collected and sonicated in RIPA lysis buffer (Beyotime, P0013B) on ice for protein extraction. The protein supernatant was collected and the concentration was determined by BCA protein assay kit (Beyotime, P0012). Total protein (20  $\mu$ g) was analyzed by SDS-PAGE and then transferred to NC membranes. The NC membranes were placed in 5% skim milk and blocked at 25°C for 1 hr and then cleaned with PBST. The required blots were cut off and placed in the corresponding antibody for overnight incubation. The  $\beta$ -tubulin antibody, CST, #86298, TGF- $\beta$ 1 antibody, Abcam, ab215715, N-cadherin antibody, Proteintech, Cat No. 66219-1-Ig, E-cadherin antibody, Proteintech, Cat No.60335-1-Ig, ZO-1 antibody, Proteintech, Cat No. 21773-1-AP, Vimentin antibody, Proteintech, Cat No. 10366-1-AP, HRP\* Goat Anti Mouse IgG(H+L), Immunoway, RS0001, HRP\* Goat Anti Rabbit IgG(H+L), Immunoway, RS0002). The blots were cleaned with Phosphate Buffer Solution-Tween 20 (PBST) for several times and incubated in HRP labeled secondary antibodies at 25°C for 2 hrs. Finally, ECL luminescence detection reagent (NcmECL High, P2300) was applied to the blots and visualized in the developing instrument. ImageJ software (Fiji) was used to analyze the gray value of the film.

**Statistical analysis:** The Graph pad Prism 8.4 version software and SPSS 25.0 version software were used for data analysis. Measurement data were expressed as Mean  $\pm$  SD. Two-way

ANOVA was used to analyze the results of multiple groups and One-way ANOVA or two-tailed student's T-test were used to compare between groups. Among all the statistical results,  $p<0.05$  was considered statistically significant.

**RESULTS****Results of *in vivo* analysis**

**Validation of animal models:** The tumor growth of mice in the Tumor group and the Tumor+CUMS group could be gradually detected about 21 days after LLC cells were inoculated subcutaneously. Compared with the Control group, the total distance of movement and the total distance of movement in the central area in OFT was significantly reduced in CUMS group and Tumor+CUMS group ( $p<0.05$ ) and the times of entering the central area was significantly reduced after 6 weeks of chronic stress ( $p<0.01$ ) (Fig. 1a-d). In TST, compared with the Control group, the immobile time of CUMS group mice was extended ( $p<0.05$ ) and the immobile time of tumor mice was also extended. Compared with the Tumor group, the immobile time of the Tumor+CUMS group was significantly extended ( $p<0.05$ ) (Fig. 1e). In the FST, the immobile time of mice in CUMS group was prolonged and the immobile time of mice in Tumor+CUMS group was also prolonged ( $p<0.05$ ). Compared with the Tumor group, the immobile time of Tumor+CUMS group was significantly extended ( $p<0.05$ ) (Fig. 1f). Compared with the Control group, the sucrose preference of CUMS group and Tumor+CUMS group was significantly decreased ( $p<0.05$ ). Compared with mice in Tumor group, the sucrose preference of mice in Tumor+CUMS group was significantly decreased ( $p<0.05$ ) (Fig. 1g). Behavioral tests (OFT, TST and FST) and sucrose preference test results indicated that the chronic stress induced depression-like phenotype mice and tumor comorbidities depression model was successfully established.

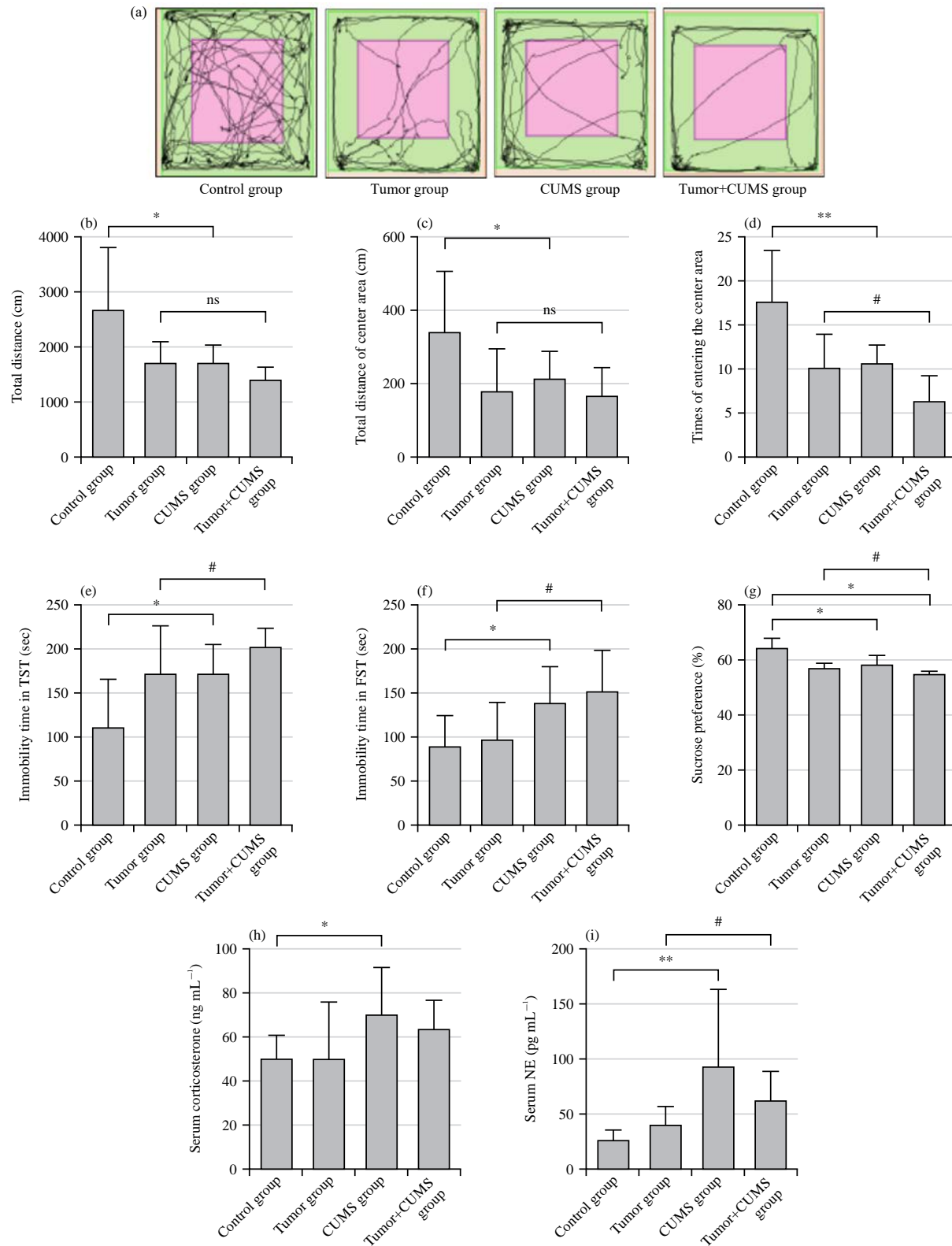


Fig. 1(a-i): Validation of animal models, (a) Motion track, (b) Total distance in OFT, (c) Total distance of center area, (d) Times of entering the center area, (e) TST, (f) FST, (g) Sucrose preference percentage, (h) Serum corticosterone level and (i) Serum NE level

\*p<0.05 vs Control group, \*\*p<0.01 vs Control group and #p<0.05 vs Tumor group

**Serum corticosterone and norepinephrine assay:** After chronic stress, the serum corticosterone level of mice was increased ( $p<0.05$ ). Compared with the Tumor group, the serum corticosterone level of mice in Tumor+CUMS group was not significantly increased (Fig. 1h). After chronic stress, the serum norepinephrine level of mice was increased ( $p<0.01$ ). Compared with normal Control group, the serum norepinephrine level of mice in Tumor group and the Tumor+CUMS group was significantly increased ( $p<0.05$ ) and the serum norepinephrine level of mice in Tumor+CUMS group was significantly increased compared with that in Tumor group ( $p<0.05$ ) (Fig. 1i).

**Chronic stress promotes tumor growth:** About 21 days after LLC cells were subcutaneously inoculated in mice in the Tumor group and the Tumor+CUMS group, tumor growth was gradually observed. As shown in Fig. 2a-b, about 11 days after tumor growth, the tumor growth rate of mice in the Tumor+CUMS group was accelerated ( $p<0.05$ ) and the overall tumor volume was higher than that in the Tumor group in 17 day after tumor development ( $p<0.05$ ). During modeling, the weight of four groups of mice were recorded every 7 days. Compared with the Control group, the weight of mice in Tumor+CUMS group increased slowly. There was no significant difference in body weight among the other groups (Fig. 2c).

**Liver and lung lesions in model mice:** After the modeling, no lung cancer metastasis was observed in the abdominal cavity and lung tissues of the mice, while metastatic nodules were found on the liver of the tumorous mice. White nodules were visible on the liver lobes of mice in the Tumor group and the Tumor+CUMS group, while the number of nodules in the liver in the Tumor+CUMS group was more than that in the Tumor group (Fig. 2d).

In HE staining of mouse liver sections, liver cords of mice in the Control group were arranged neatly (red arrow), cell sizes varied and a small amount of inflammatory cell infiltration was observed (purple arrow). The liver cords of mice in the Tumor group were not neatly arranged, lipid droplet (black arrow) could be seen in the community, liver cells were cloudy (yellow arrow) and occasionally balloon-like transformation (green arrow) could be seen. In the CUMS group, the hepatic cords were not neatly arranged, the hepatocytes were cloudy and the interstitial Kupffer cells (hepatic macrophages) were hyperplasia (brown arrow). The liver of mice in the Tumor+CUMS group was disordered, hepatocytes were cloudy with disappearance of hepatocytes

(blue arrow), interstitial Kupffer cells proliferated and a large number of inflammatory cells infiltrated (purple arrow) (Fig. 2e).

In the lung HE staining, compared with the Control group, the alveolar structure of mice in the Tumor group, CUMS group and Tumor+CUMS group was indistinct and there were a large number of inflammatory cells exuding in the airway, adjacent to the air passage, beside the blood vessels and alveoli in the lung tissue (black arrow) and the alveolar interval in some areas was widened (red arrow). A large number of lymphocytes gathered in the lung tissue in the Tumor group. In addition, compared with the Tumor group, the structure of the alveolar space of mice in the Tumor+CUMS group was blurring, the alveolar space of the lung tissue was significantly widened, part of the alveolar space was broken and cancer cells were transferred to the vasculature (green arrow) (Fig. 2f).

**Analysis of EMT relative mRNA and proteins *in vivo*:** The expression of TGF- $\beta$ 1 associated with tumor progression in the liver of four groups of mice were estimated, as well as the expression of proteins associated with EMT. The result of WB showed that the expression of TGF- $\beta$ 1 in liver tissues of mice in the Tumor group and the Tumor+CUMS group was increased (Fig. 3a-b). Results speculated that the high expression of TGF- $\beta$ 1 in liver affected the progression of tumor. The EMT related protein expression was analyzed in the liver of mice in the Tumor group and the Tumor+CUMS group. According to the results, epithelial molecular markers E-cadherin and ZO-1 were down-regulated in the Tumor+CUMS group, compared with those in the Tumor group ( $p<0.01$ ). The expression of interstitial molecular marker N-cadherin and Vimentin were up-regulated ( $p<0.05$ ) (Fig. 3c-d). Subsequently, protein analysis was conducted on tumor tissues of the two groups of tumor-bearing mice and it was found that the expression of TGF- $\beta$ 1 in tumor tissues of mice in the Tumor+CUMS group was increased compared with those in the Tumor group ( $p<0.01$ ) (Fig. 3e-f). In addition, compared with the Tumor group, the expressions of E-cadherin and ZO-1 in the Tumor+CUMS group were decreased ( $p<0.01$ ), while the expressions of N-cadherin ( $p<0.01$ ) and Vimentin ( $p<0.05$ ) were increased (Fig. 3g-h), conforming to the conjecture that the up-regulation of TGF- $\beta$ 1 promotes the progression of EMT. Compared with the Tumor group, the mRNA expressions of E-cadherin and ZO-1 in the Tumor+CUMS group were down-regulated ( $p<0.05$ ), while the mRNA expressions of TGF- $\beta$ 1 ( $p<0.05$ ) N-cadherin ( $p<0.01$ ) and Vimentin ( $p<0.01$ ) were up-regulated (Fig. 3i).

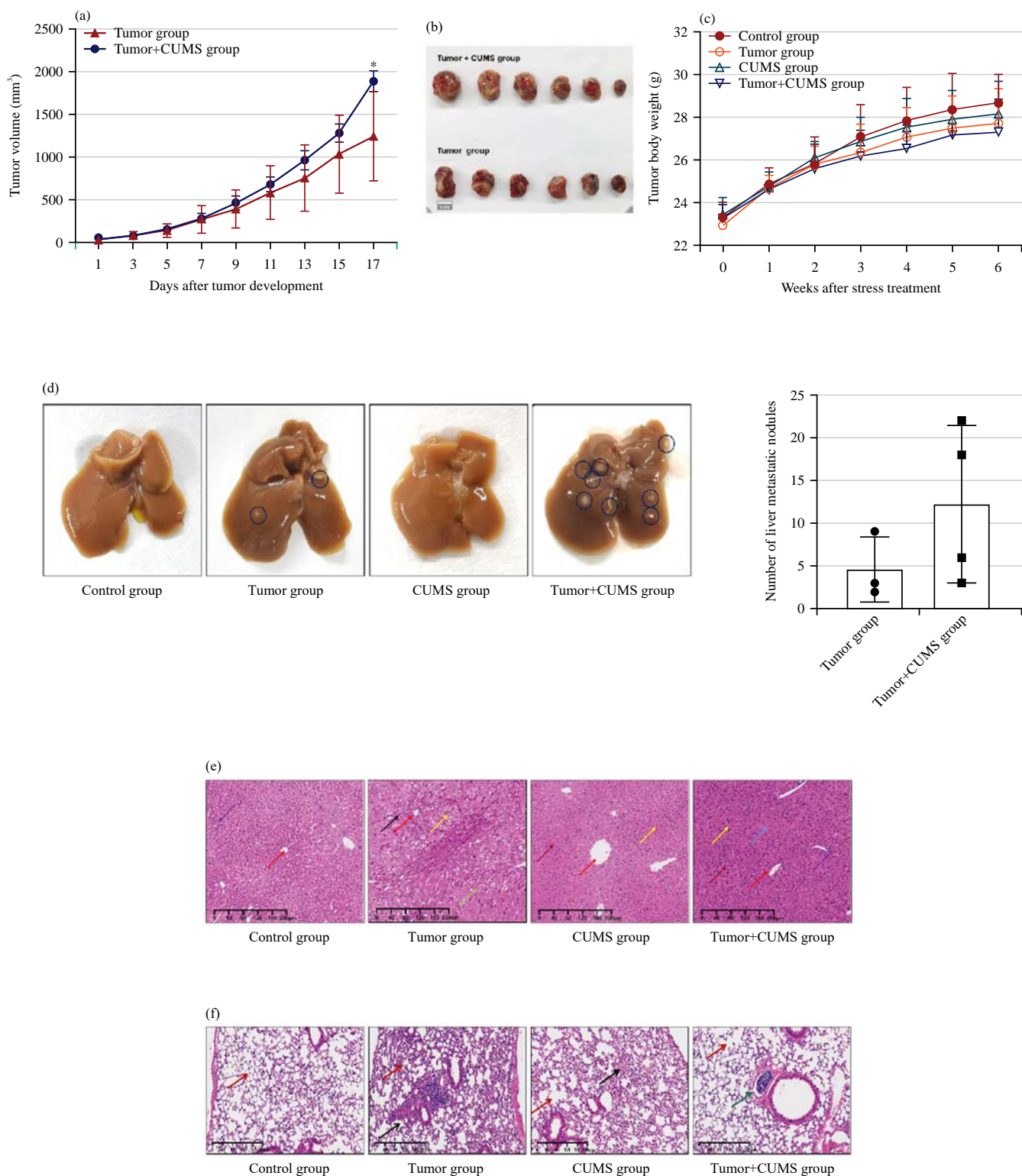


Fig. 2(a-f): Chronic stress promotes tumor growth, (a) Tumor growth curve of tumor-bearing mice, (b) Images of tumor, (c) Growing body weight of mice during modeling (n = 8/group), (d) Liver anatomy of different groups of mice, (e) H&E staining of liver tissue in each group (100×) and (f) H&E staining of liver tissue in each group (100×)  
 (a) \*p<0.05 vs Tumor group on day 17 and (c) \*p<0.05 vs Control group

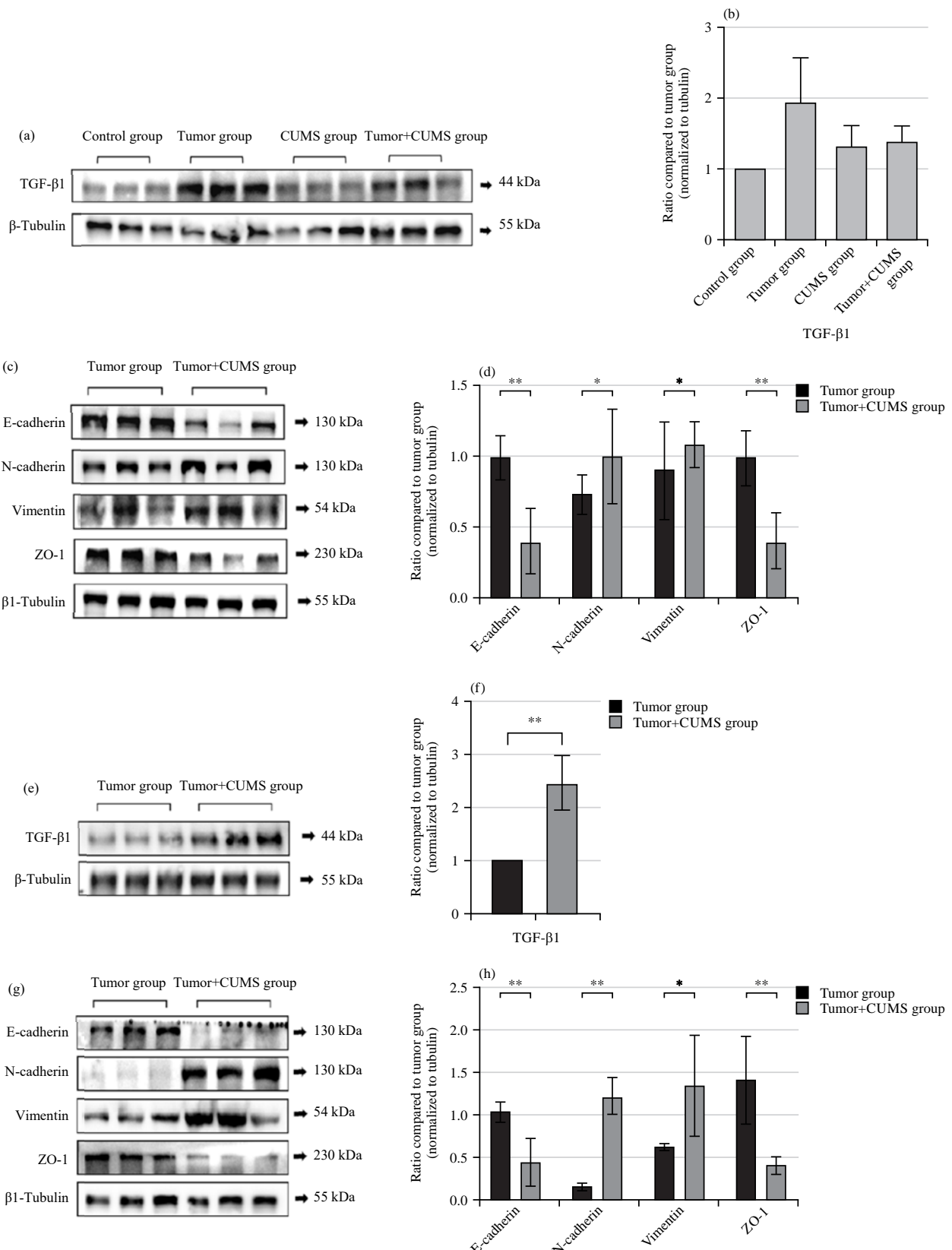


Fig. 3(a-i): Continue

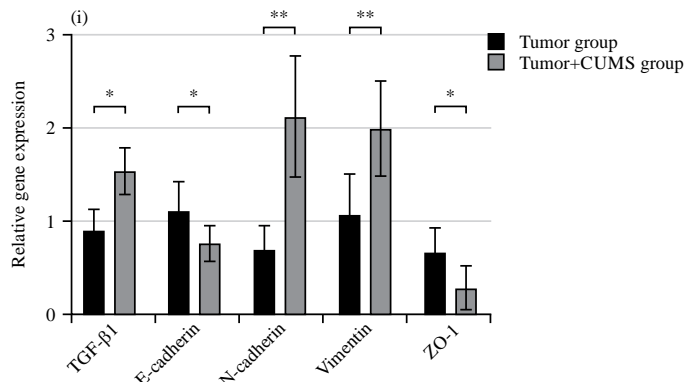


Fig. 3(a-i): Analysis of EMT relative mRNA and proteins *in vivo*, (a) Expression of TGF-β1 protein in liver of mice in each group (n = 3/group), (b) Gray values of (a), (c) Expression of EMT proteins in liver of mice in Tumor group and Tumor+CUMS group (n = 3/group), (d) Gray values of (c), (e) Expression of TGF-β1 in tumor of mice in Tumor group and Tumor+CUMS group (n = 3/group), (f) Gray values of (e), (g) Expression of EMT proteins in tumor of mice in Tumor group and Tumor+CUMS group (n = 3/group), (h) Gray values of (g) and (i) Relative gene expression of EMT in mouse tumor (n = 3/group)

\*p<0.05 and \*\*p<0.01 vs Tumor group

### Results of *in vitro* analysis

#### Cell proliferation, migration and invasion under CORT and NE:

The CCK8 results show that A549 cell had a high proliferation activity when exposed to 1.5 μM CORT for 24 hrs (p<0.05) and to 10 μM NE for 48 hrs (p<0.01) (Fig. 4a). Cell morphology was changed under 1.5 μM CORT and 10 μM NE. In the Control group, cytoskeleton protein (actin) was mainly distributed in the perimembrane. However, the actin in the perimembrane gradually decreased when exposed to CORT, while the actin in the cytoplasm increased, accompanied by the increase of stress fibers. The cell morphology changed like fiber with invasion characteristic under NE (Fig. 4b). In cell cloning, compared with the Control group, A549 cells formed colony number increased significantly when cultured 1.5 μM CORT and 10 μM NE (p<0.01) (Fig. 4c). Compared with the Control group, in 1.5 μM CORT and 10 μM NE, A549 cell showed a scratched narrowed considerably, cell migration speed (p<0.05), at 48 hrs, the scratches of cells treated with 10 μM NE almost healed, indicating that CORT and NE promoted the horizontal migration ability of A549 cells (Fig. 4d-e). In cell migration and invasion, the number of cell migration and invasion under the treatment of 1.5 μM CORT and 10 μM NE was significantly higher than that in the Control group (p<0.01), which significantly enhanced the ability of cell migration and invasion (Fig. 4f-g).

#### Cell migration and invasion in response to CORT and NE after knockdown TGF-β1:

In order to verify whether stress hormones promote EMT process by inducing TGF-β1, small interfering RNA (siRNA) was used to knock down TGF-β1 in A549 cells and then cultured the cells in 1.5 μM CORT and 10 μM NE. Compared with the Control group, the number of cell migration was significantly increased when CORT and NE were applied (p<0.01). The number of cell migration was significantly decreased in siTGF-β1 group than NC group (p<0.01), while the number of cell migration increased when exposed to 1.5 μM CORT and 10 μM NE (p<0.05) (Fig. 5a-b) and the cell invasion results were similar to the migration results (Fig. 5c-d).

#### Analysis of EMT relative mRNA and proteins *in vitro*:

The A549 cells treated with 1.5 μM CORT and 10 μM NE showed increased the gene and protein expression of TGF-β1, N-cadherin and Vimentin, while decreased the gene and protein expression of E-cadherin and ZO-1 (Fig. 6a-c). Compared with the NC group, the mRNA and protein expressions of E-cadherin and ZO-1 in group transfected with siRNA-TGF-β1 were increased and the expressions of N-cadherin and Vimentin were decreased. However, compared with the group transfected with siRNA-TGF-β1 (siTGF-β1 group), the mRNA and protein expressions of TGF-β1 increased when exposing to

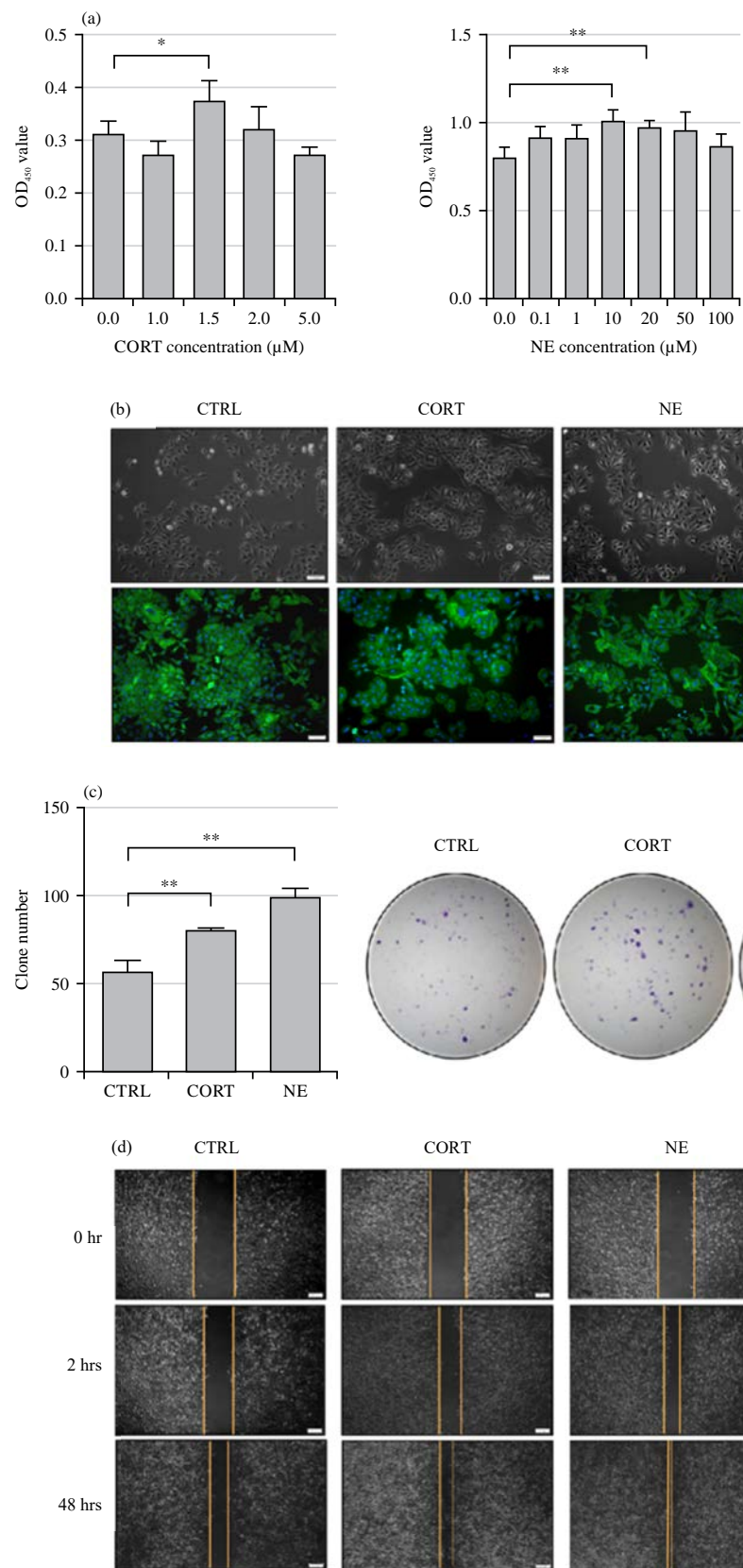


Fig. 4(a-g): Continue

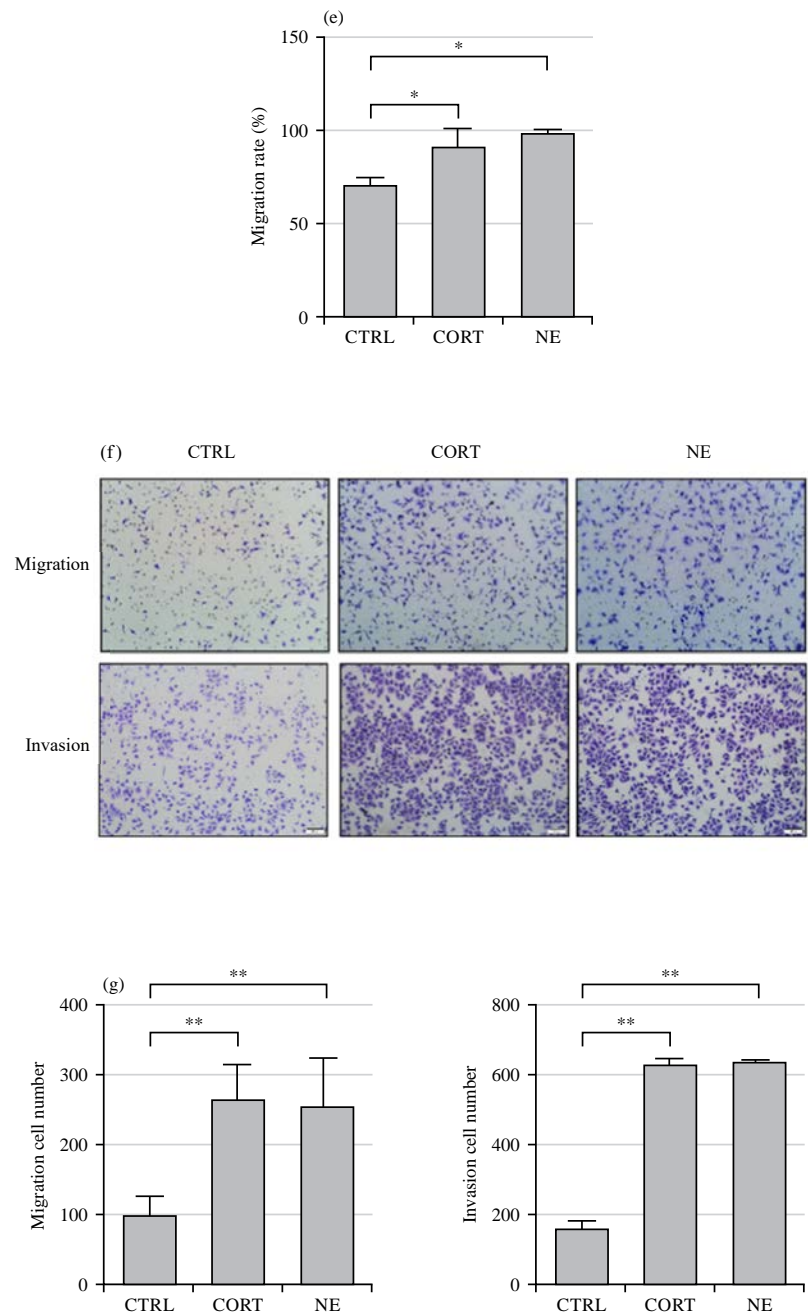


Fig. 4(a-g):Cell proliferation, migration and invasion under CORT and NE, (a) CCK-8, (b) Cell morphology (100 $\times$ ), (c) Colony formation assay, (d) Cell wound healing assay (100 $\times$ ), (e) Migration rate of cell wound healing assay, (f) Cell migration and invasion (100 $\times$ ) and (g) Migration and invasion cell number  
\*p<0.05 and \*\*p<0.01 vs Control group

CORT and NE siTGF- $\beta$ 1+CORT group and siTGF- $\beta$ 1+NE group ( $p<0.01$ ). The change of gene and protein of EMT were reversed exposing cell with siTGF- $\beta$ 1 to CORT and NE, showed that the mRNA and protein expression of E-cadherin and ZO-1 were down-regulated ( $p<0.05$ ) and

expressions of N-cadherin and Vimentin were up-regulated ( $p<0.05$ ) (Fig. 6d-e). To sum up, current study results implied the critical role of TGF- $\beta$ 1 in tumor comorbidity depression, promoting tumor EMT and affecting tumor progression.

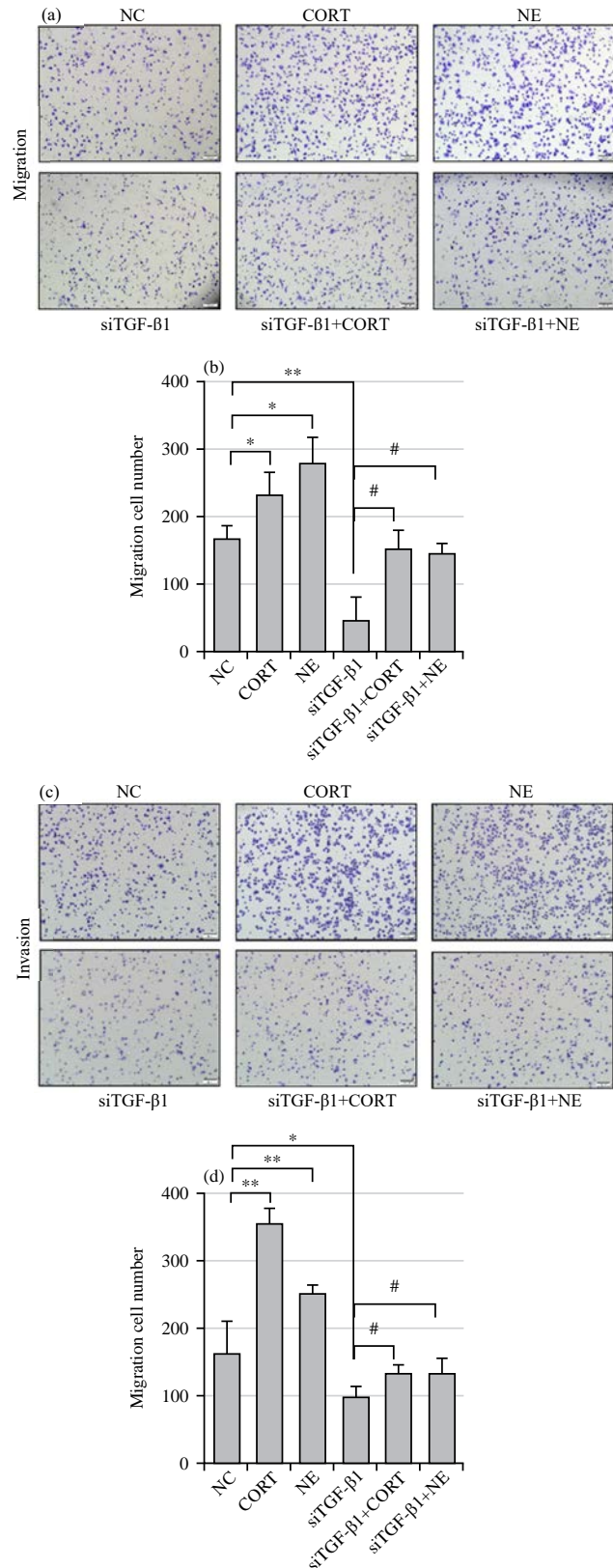


Fig. 5(a-d): Cell migration and invasion after transfection, (a) Cell migration after transfection (100 $\times$ ), (b) Migration cell number after transfection, (c) Cell invasion after transfection (100 $\times$ ) and (d) Invasion cell number after transfection  
 $*p<0.05$ ,  $**p<0.01$  vs CTRL/NC and  $#p<0.05$  vs si-TGF- $\beta$ 1

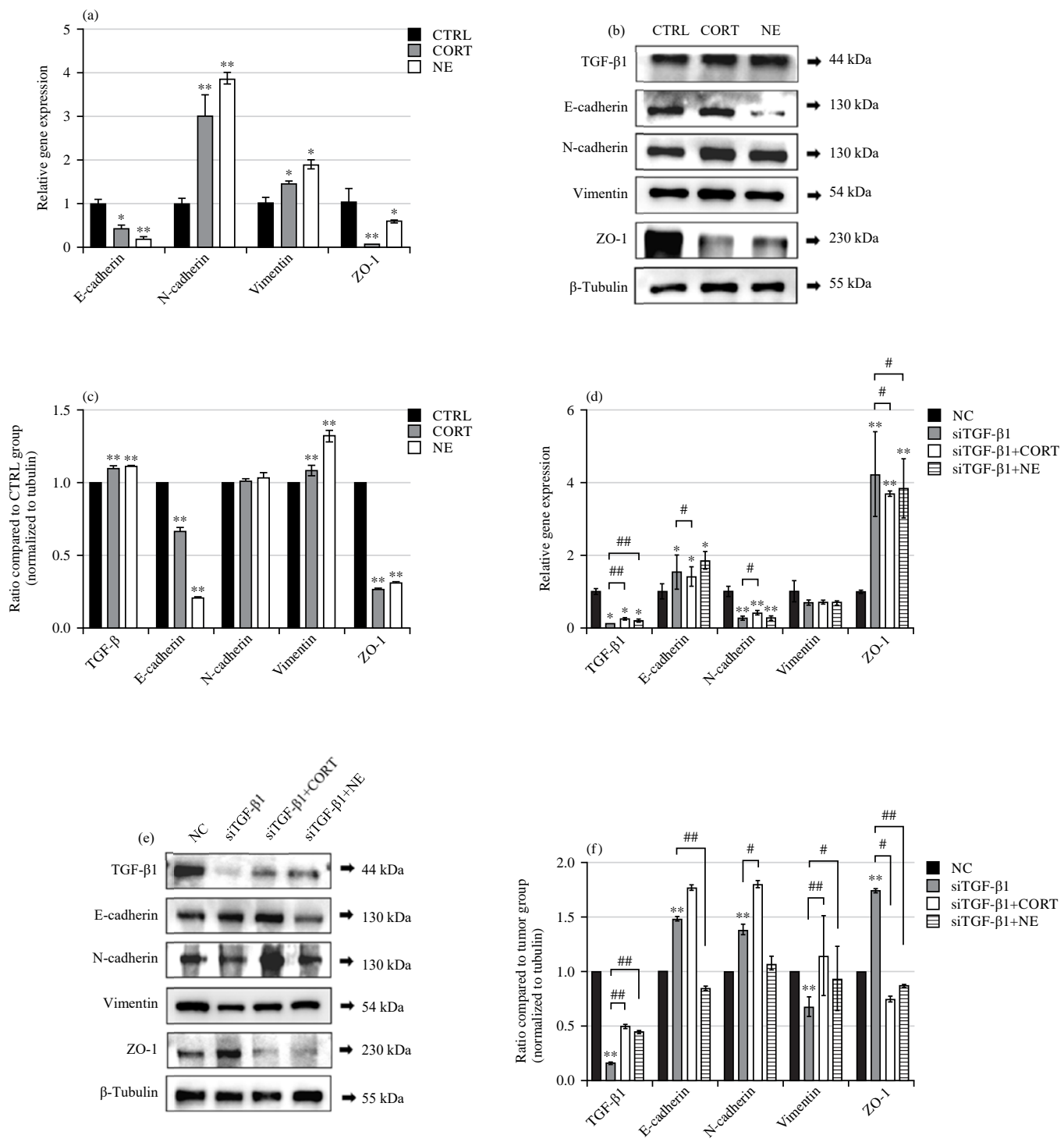


Fig. 6(a-f): Analysis of EMT relative mRNA and proteins *in vitro*, (a) Expression of EMT-related molecular genes in cells treated with CORT and NE, (b) Expression of EMT-related molecular proteins in cells treated with CORT and NE, (c) Gray values of (b), (d) Expression of EMT-related molecular genes in cells treated with siRNA, (e) Expression of EMT-related molecular proteins in cells treated with siTGF-β1 and (f) Gray values of (e)

\*p<0.05, \*\*p<0.01 vs CTRL/NC and #p<0.05 vs si-TGF-β1

## DISCUSSION

Cancer is a major public health problem and the lung cancer deaths are a significant proportion of cancer deaths in the world<sup>7</sup>. More and more studies show that chronic stress, such as physiological and psychological, affects the progression of cancer and cancer is more likely to lead to depression. In this study, a tumor-bearing mouse model was constructed by translocation inoculation of tumor cells, a depression-like phenotype mouse model was constructed by chronic unpredictable mild stress (CUMS) and a Tumor+CUMS mouse model was constructed by comorbidities. In the comorbidity model, LLC lung cancer cells were injected subcutaneously into the posterior right limb of mice and then the chronic stress model was constructed for 6 weeks to simulate the fact that clinically depressed patients with cancer comorbidity are caused by cancer and then depression or that patients themselves carry susceptibility genes and then depression caused by psychological stress leads to cancer. About 21 days after the injection of LLC cells, tumor development was gradually observed. In CUMS, the mice subjected to chronic stress showed decreased sucrose preference and reduced activity in OFT. In TST and FST, the time of condition of rest after chronic stress was prolonged, indicating that the chronic stress caused the mice a psychology similar to despair, indicating that the depression-like phenotype mouse model was successfully constructed. In addition, we found that mice in the tumor group also showed decreased preference for sucrose water, reduced total distance and prolonged the time of immobility, which can be inferred that the occurrence of tumor also leads to the generation of depression and this phenomenon was more obvious in mice of Tumor+CUMS group, indicating that chronic stress aggravates the depression of tumor bearing mice.

From tumor pictures, it was concluded that chronic stress promotes tumor progression in mice. In the follow-up experiment, it was found that chronic stress led to the increase of serum levels of stress hormones CORT and NE and inflammation in the body. The liver nodules of co-morbidities mice were more than those of mice in the simple tumor bearing group and the metastasis of cancer cells was inclined to occur. Tumor cells in the body will have nearby metastasis, invasion or cancer cells into the blood for blood route metastasis, which speculated that chronic stress caused immune disorders and inflammatory responses, providing an environment for tumor progression.

When cancer patients learn about their own disease and bear the physical and psychological burden as well as the economic burden, they often suffer from chronic stress caused by psychological disorders<sup>31</sup>. Social stress is associated with increased lung cancer incidence and mortality<sup>31,32</sup>. Chronic stress activates the neuroendocrine pathway HPA axis and SNS, up-regulates the secretion of various stress hormones, inhibits cellular immunity and induces chronic inflammation, thus affecting the body's immune system and regulating multiple signaling pathways to promote tumor development<sup>14,33-35</sup>. In various cancers, chronic exposure to stress-related hormones encourages tumor growth, invasion and angiogenesis<sup>36</sup>. Neuroendocrine changes caused by stress affect tumor progression, which is a major health problem that has attracted much attention in recent years.

Inflammation can increase the risk of cancer by providing bioactive molecules that infiltrate the tumor microenvironment, including cytokines, growth factors, chemokines that maintain a sustained proliferation rate, cell survival signals to avoid apoptosis and pro-angiogenic factors<sup>37-39</sup>. Depressed patients often display high levels of pro-inflammatory cytokines in their bodies<sup>40,41</sup>.

In this study, TGF- $\beta$ 1 was highly expressed in liver tissues of cancer mice. The expression of TGF- $\beta$ 1 in comorbidities depression mice was higher than that in tumor mice and the results of EMT-related molecular analysis were consistent with the fact that chronic stress promoted the EMT process. *In vivo*, the morphology of A549 cells changed when exposed to CORT and NE, while the cytoplasmic actin increased, accompanied by increased stress fibers, which supported the development of EMT. The results of functional experiments showed that the colony formation, migration and invasion of A549 cells were enhanced after treatment with CORT and NE. The protein expressions of TGF- $\beta$ 1 were increased, the mRNA and protein of N-cadherin and Vimentin were increased, while E-cadherin and ZO-1 were decreased. After the knockdown of TGF- $\beta$ 1, the migration and invasion ability of A549 cells were diminished. The mRNA and protein expressions of N-cadherin and Vimentin proteins were down-regulated, while the expressions of E-cadherin and ZO-1 were up-regulated, suggesting that TGF- $\beta$ 1 was involved in tumor progression. However, when the cells with knockdown of TGF- $\beta$ 1 were exposed to CORT and NE and its migration and invasion ability were enhanced additionally and reversed the molecular level changes which appeared when knocking down TGF- $\beta$ 1.

The occurrence, development, migration, invasion and metastasis of tumor is a complex process, involving the remodeling of intercellular skeleton and the change of intercellular adhesion. One vital molecular mechanism promoting the progression of metastasis is epithelial-mesenchymal transition (EMT), a pathological process leading to tumor progression, which drives the invasion and migration of various cancers<sup>42,43</sup>. Under the action of some factors, epithelial cells lose their polarity, tight junctions and adhesion junctions between cells, gain the ability to infiltrate and migrate and become cells with the morphology and characteristics of interstitial cells, which may also induce escape apoptosis of tumor cells<sup>19,20</sup>. In the study of tumor, the occurrence of EMT indicates the malignant process of tumor. The TGF- $\beta$  (Transforming Growth Factor- $\beta$ ) is a multifunctional cytokine that plays a bidirectional regulatory role in tumor progression. The TGF- $\beta$  is a potential tumor suppressor in the early stages of tumorigenesis. With the progression of tumor, TGF- $\beta$  is transformed into tumor promoting factor to promote tumor metastasis<sup>44,45</sup>. In pathological conditions, TGF- $\beta$  overexpression leads to EMT, extracellular matrix deposition and cancer-associated fibroblast formation, leading to cancer and fibrotic diseases<sup>46</sup>. It was found that inhibition of TGF- $\beta$ 1/Smad2/3/Foxp3 signaling pathway can attenuate the protein expression of lymphocyte apoptosis and apoptosis-related induced of chronic stress and restored the imbalance between chronic stress-induced pro-inflammatory cytokines and anti-inflammatory cytokines<sup>47</sup>. It is suggested that TGF- $\beta$ 1 pathway may be a new target for chronic stress regulation of immune function.

Therefore, the conclusion might be drawn that the high stress hormone caused by chronic stress induced the expression of TGF- $\beta$ 1, strengthening the progression of EMT and thus promoting the tumor process.

## CONCLUSION

Chronic stress led to nonstandard secretion of stress hormones CORT and NE in the body, aggravated inflammation in tissue and promotes tumor progression. Molecular mechanism studies had shown that abnormal secretion of stress hormone caused by chronic stress affected the expression of TGF- $\beta$ 1 and thus affected the tumor EMT progression. In view of the related mechanism of chronic stress promoting tumor progression, methods such as signal pathway-specific target blockers, hormone receptor blockers and psychotherapy are applied to pay attention to the mental state of cancer patients in clinical work, timely psychological

counseling is conducted to improve the chronic stress state of patients and ensure effective anti-cancer treatment and good prognosis. The research on the mechanism pathway related to chronic stress can provide a new idea for clinical antitumor therapy.

## SIGNIFICANCE STATEMENT

Since an increasing number of cancer patients suffer from comorbid depression which deteriorates their condition and quality of life, attention should be paid to this issue. This study aimed to understand whether chronic stress might promote the development of cancer. This study focused on the molecular mechanisms by which chronic stress affects tumor progression. The data showed that chronic stress leads to abnormal secretion of the stress hormones corticosterone and noradrenaline *in vivo*, exacerbates tissue inflammation and promotes tumor progression by affecting the expression of TGF- $\beta$ 1, which in turn affects the EMT progression of tumors. Current results findings may provide a new idea for the treatment of tumor-combined depression.

## REFERENCE

1. Zhao, D., Z. Wu, H. Zhang, D. Mellor and L. Ding *et al.*, 2018. Somatic symptoms vary in major depressive disorder in China. *Compr. Psychiatry*, 87: 32-37.
2. Malhi, G.S., C.M. Coulston, K. Fritz, L. Lampe and D.M. Bargh *et al.*, 2014. Unlocking the diagnosis of depression in primary care: Which key symptoms are GPs using to determine diagnosis and severity? *Aust. N. Z. J. Psychiatry*, 48: 542-547.
3. Malhi, G.S. and J.J. Mann, 2018. Depression. *Lancet*, 392: 2299-2312.
4. Thaker, P.H., S.K. Lutgendorf and A.K. Sood, 2007. The neuroendocrine impact of chronic stress on cancer. *Cell Cycle*, 6: 430-433.
5. Zhao, L., J. Xu, F. Liang, A. Li, Y. Zhang and J. Sun, 2015. Effect of chronic psychological stress on liver metastasis of colon cancer in mice. *PLoS ONE*, Vol. 10. 10.1371/journal.pone.0139978.
6. Siegel, R.L., K.D. Miller, H.E. Fuchs and A. Jemal, 2021. Cancer statistics, 2021. *CA: A Cancer J. Clinicians*, 71: 7-33.
7. Bray, F., J. Ferlay, I. Soerjomataram, R.L. Siegel, L.A. Torre and A. Jemal, 2018. Global cancer statistics 2018: GLOBOCAN estimates of incidence and mortality worldwide for 36 cancers in 185 countries. *CA: Cancer J. Clin.*, 68: 394-424.
8. Bade, B.C. and C.S.D. Cruz, 2020. Lung cancer 2020: Epidemiology, etiology, and prevention. *Clin. Chest Med.*, 40: 1-24.

9. Beratis, S., A. Katrivanou, S. Georgiou, A. Monastirli, E. Pasmatzi, P. Gourzis and D. Tsambaos, 2005. Major depression and risk of depressive symptomatology associated with short-term and low-dose interferon- $\alpha$  treatment. *J. Psychosomatic Res.*, 58: 15-18.
10. Bray, F. and Is. Soerjomataram, 2015. The Changing Global Burden of Cancer: Transitions in Human Development and Implications for Cancer Prevention and Control. In: Publication: Disease Control Priorities, Third Edition: Volume 3. Cancer, Gelband, H., P. Jha, R. Sankaranarayanan and S. Horton (Eds.), World Bank, Washington, United States, ISBN: 978-1-4648-0349-9, pp: 23-44.
11. Pinquart, M. and P.R. Duberstein, 2010. Depression and cancer mortality: A meta-analysis. *Psychol. Med.*, 40: 1797-1810.
12. Powell, N.D., A.J. Tarr and J.F. Sheridan, 2013. Psychosocial stress and inflammation in cancer. *Brain Behav. Immun.*, 30: S41-S47.
13. Yang, Z., Z. Li, Z. Guo, Y. Ren and T. Zhou *et al.*, 2021. Antitumor effect of fluoxetine on chronic stress-promoted lung cancer growth via suppressing kynurenine pathway and enhancing cellular immunity. *Front. Pharmacol.*, Vol. 12. 10.3389/fphar.2021.685898.
14. Rao, R. and I.P. Androulakis, 2019. Allostatic adaptation and personalized physiological trade-offs in the circadian regulation of the HPA axis: A mathematical modeling approach. *Sci. Rep.*, Vol. 9. 10.1038/s41598-019-47605-7.
15. Calvani, M., G. Bruno, M.D. Monte, R. Nassini and F. Fontani *et al.*, 2019.  $\beta_3$ -adrenoceptor as a potential immuno suppressor agent in melanoma. *Br. J. Pharmacol.*, 176: 2509-2524.
16. Koch, C.E., B. Leinweber, B.C. Drengberg, C. Blaum and H. Oster, 2017. Interaction between circadian rhythms and stress. *Neurobiol. Stress*, 6: 57-67.
17. Dick, T.E., Y.I. Molkov, G. Nieman, Y.H. Hsieh and F.J. Jacono *et al.*, 2012. Linking inflammation, cardiorespiratory variability, and neural control in acute inflammation via computational modeling. *Front. Physiol.*, Vol. 3. 10.3389/fphys.2012.00222.
18. Weng, C.H., L.Y. Chen, Y.C. Lin, J.Y. Shih and Y.C. Lin *et al.*, 2019. Epithelial-mesenchymal transition (EMT) beyond EGFR mutations per se is a common mechanism for acquired resistance to EGFR TKI. *Oncogene*, 38: 455-468.
19. Singh, M., N. Yelle, C. Venugopal and S.K. Singh, 2018. EMT: Mechanisms and therapeutic implications. *Pharmacol. Ther.*, 182: 80-94.
20. Davis, F.M., T.A. Stewart, E.W. Thompson and G.R. Monteith, 2014. Targeting EMT in cancer: Opportunities for pharmacological intervention. *Trends Pharmacol. Sci.*, 35: 479-488.
21. Seoane, J. and R.R. Gomis, 2017. TGF- $\beta$  family signaling in tumor suppression and cancer progression. *Cold Spring Harb. Perspect. Biol.*, Vol. 9. 10.1101/cshperspect.a022277.
22. Xu, J., S. Lamouille and R. Deryck, 2009. TGF- $\beta$ -induced epithelial to mesenchymal transition. *Cell Res.*, 19: 156-172.
23. Hao, Y., D. Baker and P.T. Dijke, 2019. TGF- $\beta$ -mediated epithelial-mesenchymal transition and cancer metastasis. *Int. J. Mol. Sci.*, Vol. 20. 10.3390/ijms20112767.
24. Chen, Y., W. Cai, C. Li, Z. Su and Z. Guo *et al.*, 2022. Sex differences in peripheral monoamine transmitter and related hormone levels in chronic stress mice with a depression-like phenotype. *PeerJ*, Vol. 10. 10.7717/peerj.14014.
25. Xu, F., Y. Ren, C. Yang, Z. Li and Z. Yang *et al.*, 2018. Chronic stress disturbs metabolome of blood plasma and urine in diabetic rats. *Front. Psychiatry*, Vol. 9. 10.3389/fpsyg.2018.00525.
26. Zhou, T., M. Li, Z. Xiao, J. Cai and W. Zhao *et al.*, 2021. Chronic stress-induced gene changes *in vitro* and *in vivo*: Potential biomarkers associated with depression and cancer based on circRNA- and lncRNA-associated ceRNA networks. *Front. Oncol.*, Vol. 11. 10.3389/fonc.2021.744251.
27. Katz, R.J., 1982. Animal model of depression: Pharmacological sensitivity of a hedonic deficit. *Pharmacol. Biochem. Behav.*, 16: 965-968.
28. Willner, P., A. Towell, D. Sampson, S. Sophokleous and R. Muscat, 1987. Reduction of sucrose preference by chronic unpredictable mild stress and its restoration by a tricyclic antidepressant. *Psychopharmacology*, 93: 358-364.
29. Antoniuk, S., M. Bijata, E. Ponimaskin and J. Włodarczyk, 2019. Chronic unpredictable mild stress for modeling depression in rodents: Meta-analysis of model reliability. *Neurosci. Biobehav. Rev.*, 99: 101-116.
30. Liu, M.Y., C.Y. Yin, L.J. Zhu, X.H. Zhu and C. Xu *et al.*, 2018. Sucrose preference test for measurement of stress-induced anhedonia in mice. *Nat. Protoc.*, 13: 1686-1698.
31. Cordova, M.J., M.B. Riba and D. Spiegel, 2017. Post-traumatic stress disorder and cancer. *Lancet Psychiatry*, 4: 330-338.
32. Yang, T., Y. Qiao, S. Xiang, W. Li, Y. Gan and Y. Chen, 2019. Work stress and the risk of cancer: A meta analysis of observational studies. *Int. J. Cancer*, 144: 2390-2400.
33. Jackson, M., 2014. The stress of life: A modern complaint? *Lancet*, 383: 300-301.
34. Filippi, L., G. Bruno, V. Domazetovic, C. Favre and M. Calvani, 2020. Current therapies and new targets to fight melanoma: A promising role for the  $\beta_3$ -adrenoreceptor. *Cancers*, Vol. 12. 10.3390/cancers12061415.
35. Thaker, P.H., L.Y. Han, A.A. Kamat, J.M. Arevalo and R. Takah *et al.*, 2006. Chronic stress promotes tumor growth and angiogenesis in a mouse model of ovarian carcinoma. *Nat. Med.*, 12: 939-944.
36. Krizanova, O., P. Babula and K. Pacak, 2016. Stress, catecholaminergic system and cancer. *Stress*, 19: 419-428.

37. Hanahan, D. and R.A. Weinberg, 2011. Hallmarks of cancer: The next generation. *Cell*, 144: 646-674.
38. Yang, C., K.J. Wardenaar, F.J. Bosker, J. Li and R.A. Schoeversl, 2019. Inflammatory markers and treatment outcome in treatment resistant depression: A systematic review. *J. Affective Disord.*, 257: 640-649.
39. Chu, A.L., M. Hickman, N. Steel, P.B. Jones, G.D. Smith and G.M. Khandaker, 2021. Inflammation and depression: A public health perspective. *Brain Behav. Immun.*, 95: 1-3.
40. Miller, A.H., V. Maletic and C.L. Raison, 2009. Inflammation and its discontents: The role of cytokines in the pathophysiology of major depression. *Biol. Psychiatry*, 65: 732-741.
41. Maes, M., 1999. Major Depression and Activation of The Inflammatory Response System. In: *Cytokines, Stress, and Depression*, Dantzer, R., E.E. Wollman and R. Yirmiya (Eds.), Springer, New York, ISBN: 978-0-585-37970-8, pp: 25-46.
42. Thiery, J.P., 2002. Epithelial-mesenchymal transitions in tumour progression. *Nat. Rev. Cancer*, 2: 442-454.
43. Gonzalez, D.M. and D. Medici, 2014. Signaling mechanisms of the epithelial-mesenchymal transition. *Sci. Signal.*, Vol. 7. 10.1126/scisignal.2005189.
44. Lu, Z., Y. Li, Y. Che, J. Huang and S. Sun *et al*, 2018. The TGF $\beta$ -induced lncRNA TBILA promotes non-small cell lung cancer progression *in vitro* and *in vivo* via cis-regulating HGAL and activating S100A7/JAB1 signaling. *Cancer Lett.*, 432: 156-168.
45. Drabsch, Y. and P. ten Dijke, 2012. TGF- $\beta$  signalling and its role in cancer progression and metastasis. *Cancer Metastasis Rev.*, 31: 553-568.
46. Peng, D., M. Fu, M. Wang, Y. Wei and X. Wei, 2022. Targeting TGF- $\beta$  signal transduction for fibrosis and cancer therapy. *Mol. Cancer*, Vol. 21. 10.1186/s12943-022-01569-x.
47. Zhang, H., Y. Caudle, C. Wheeler, Y. Zhou, C. Stuart, B. Yao and D. Yin, 2018. TGF- $\beta$ 1/Smad2/3/Foxp3 signaling is required for chronic stress-induced immune suppression. *J. Neuroimmunol.*, 314: 30-41.